iScience

CellPress
OPEN ACCESS

Article

High paternal homocysteine causes ventricular septal defects in mouse offspring

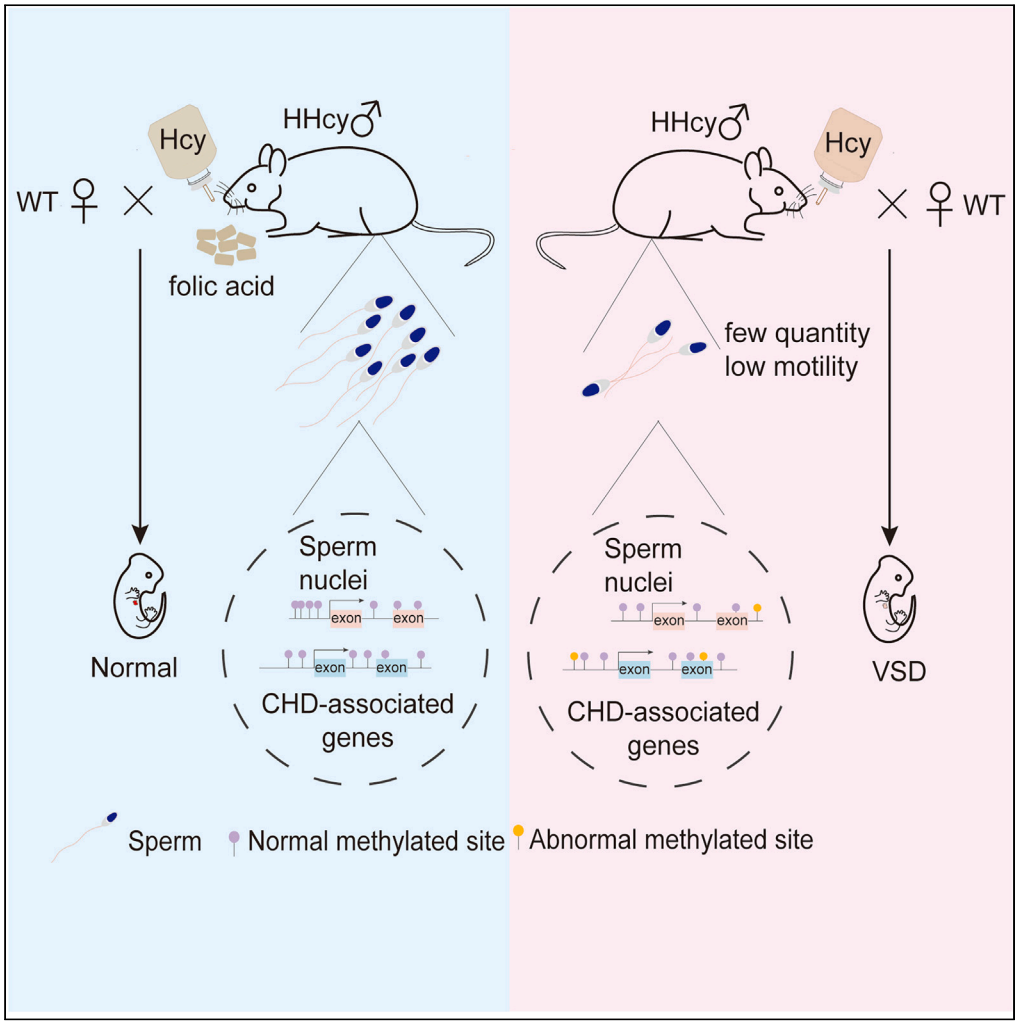

Lian Liu, Xuan Zhang, Hao-Ran Geng, Ya-Nan Qiao, Yong-Hao Gui, Jian-Yuan Zhao

yhgui@fudan.edu.cn (Y.-H.G.)
zhaojy@vip.163.com (J.-Y.Z.)

Highlights

Increased levels of homocysteine caused decreased sperm counts and sperm motility defects

Paternal high Hcy caused high risk of ventricular septal defect in offspring

Paternal high Hcy affected sperm CHD-related DNA methylation

Folic acid supplement could prevent paternal high Hcy-caused CHD

Liu et al., iScience 27, 109447
April 19, 2024
https://doi.org/10.1016/j.isci.2024.109447

iScience

CellPress
OPEN ACCESS

Article

High paternal homocysteine causes ventricular septal defects in mouse offspring

Lian Liu,[1,4] Xuan Zhang,[1,4] Hao-Ran Geng,[2,3] Ya-Nan Qiao,[2] Yong-Hao Gui,[1,*] and Jian-Yuan Zhao[3,5,*]

SUMMARY

Maternal hyperhomocysteinemia is widely considered as an independent risk of congenital heart disease (CHD). However, whether high paternal homocysteine causes CHD remains unknown. Here, we showed that increased homocysteine levels of male mice caused decreased sperm count, sperm motility defect and ventricular septal defect of the offspring. Moreover, high levels of paternal homocysteine decrease sperm DNMT3A/3B, accompanied with changes in DNA methylation levels in the promoter regions of CHD-related genes. Folic acid supplement could decrease the occurrence of VSD in high homocysteine male mice. This study reveals that increased paternal homocysteine level increases VSD risk in the offspring, indicating that decreasing paternal homocysteine may be an intervening target of CHD.

INTRODUCTION

It is well known that paternal health status has a great responsibility of offsprings' health. In addition to genetic diseases, to date, many studies have indicated paternal obesity, tobacco smoke, and exposure drugs or chemical agents have a significant impact on offspring health condition.[1–5]

Epigenetic inheritance is increasingly recognized as the one of main mechanism of paternal intergenerational and transgenerational inheritance. Spermatozoa unique epigenetic signatures contain DNA methylation profile,[6] histone modification,[7] non-coding RNA,[8] and other properties (for example, non-histone protein modification). However, there is sperm-specific situation that approximately 85% of DNA-binding histones are replaced by protamines during the elongating spermatid stage of spermatogenesis.[9,10] Most histone modifications are lost with protamines replacement so that epigenetic landscape alters simultaneously. In contrast, DNA methylation is relatively stable and has been a hot research area of paternal epigenetic inheritance until now.[5,11,12]

Homocysteine (Hcy) is one of non-protein synthesis amino acid, which is an important intermediate product in the metabolism of methionine, and its synthesis depends on methionine transmethylation (Figure 1). A high circulating concentration Hcy is a significant and independent risk factor for cardiovascular disease, like coronary artery disease and stroke.[13,14] Clinical trials have demonstrated that maternal Hcy was closely associated with congenital heart defect (CHD) and neural tube defect (NTD), and was considered as an abnormal maternal biomarker.[15–17] Moreover, animal experiments revealed maternal hyperhomocysteinemia could induce CHD such as ventricular septal defect(VSD).[18]

Investigations revealed that the prevalence of hyperhomocysteinemia for men was higher than that for women.[19,20] A large proportion of men with hyperhomocysteinemia are of childbearing age. Whether paternal hyperhomocysteinemia has effects on offspring health has not been settled down, we performed a first study to test the hypothesis that paternal hyperhomocyteinemia before mating contributed to the onset of CHD in the offspring.

RESULTS

High Hcy caused decreased sperm counts and sperm motility defects

Normal levels of blood Hcy are 10–12 μmol/L, while a level above 15 μmol/L is considered as hyperhomocysteinemia. To investigate whether a 25%–50% variation in Hcy concentration influences the quantity or vitality of sperms, we increased levels of paternal Hcy in male mice and isolated their sperms. Referring to the previous study, 2 g/L high-Hcy water was fed to Wild-type C57BL/6J male mice to generate hyperhomocysteinemia mouse model,[21] starting at weaning (4 weeks of age). After 9–11 weeks (spanning over two cycles of spermatogenesis), we

[1]Children's Hospital of Fudan University and Shanghai Genitourinary Cancer Institute Fudan University, Department of Urology, Fudan University Shanghai Cancer Center, Shanghai 201102, China
[2]School of Life Sciences, Fudan University, Shanghai 200438, China
[3]Institute for Developmental and Regenerative Cardiovascular Medicine, MOE-Shanghai Key Laboratory of Children's Environmental Health, Xinhua Hospital, Shanghai Jiao Tong University School of Medicine, Shanghai 200092, China
[4]These authors contributed equally
[5]Lead contact
*Correspondence: yhgui@fudan.edu.cn (Y.-H.G.), zhaojy@vip.163.com (J.-Y.Z.)
https://doi.org/10.1016/j.isci.2024.109447

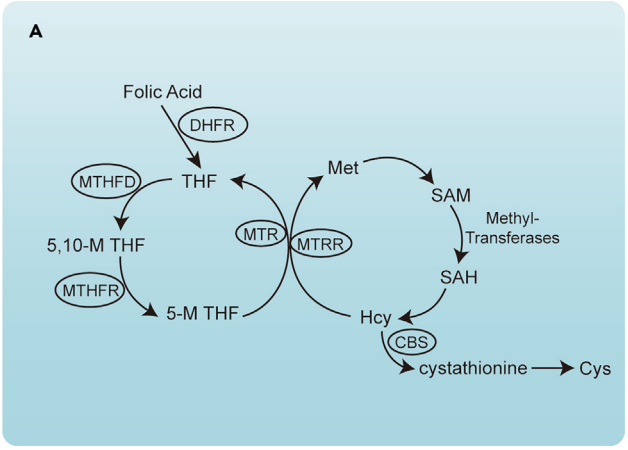

Figure 1. Methionine cycle/transmethylation and transulfuration-dependent homocysteine synthesis

(A) DHFR, dihydrofolate reductases; THF, tetrahydrofolic acid; MTHFD, Methylenetetrahydrofolate dehydrogenase; MTHFR, 5,10-methylenetetrahydrofolate reductase; MTR, 5-methyltetrahydrofolate-homocysteine methyltransferase; MTRR, 5-methyltetrahydofolate-homocysteine methyltransferase reductase; CBS, cystathionine beta-synthase.

confirmed that the plasma Hcy concentration in high-Hcy-fed mice (18.90 ± 1.25 μmol/L) increased by 50%, compared to that of control mice (12.48 ± 1.33 μmol/L) (Figure 2A).

The process of spermatogenesis and spermatozoa maturation take place in the testis and epididymis.[22] Therefore, we first dissected testes and epididymides and conducted morphology analyses between two groups. The results showed that there was no significant difference of size (Figures 2B and 2C), and histological study displayed that sperm cells at different spermatogenesis stages in two group were orderly distributed in the epithelium of the seminiferous tubules (Figure 2D). Next, we compared the testis weight and testis body weight ratio of two groups. The two sets of figures were also not significantly different regardless of left or right side (Figures 2E and 2F). Lastly, sperm was obtained from the tail of epididymis for morphology and sperm-specific analysis. In the aspect of morphology, no detectable differences between control and high-Hcy male mice were found (Figure 2G). However, sperm concentration, total motility, average path velocity, progressive velocity and curvilinear velocity, as sperm-specific analysis key parameters were analyzed using a computer-assisted sperm analysis system, and results showed that increased Hcy levels significantly reduced sperm counts and caused sperm motility defects (Figure 2H). Together, these observations indicated that high Hcy caused decreased sperm counts and sperm motility defects.

Paternal high Hcy caused ventricular septal defect of offspring

To explore transgenerational effect of paternal high Hcy, we mated high-Hcy or control male mice with normal female C57BL/6J mice to obtain F1 offspring. First, we recorded absorption rate of embryo in two groups. The results showed that absorption rates were 1.41% in F1 embryo from normal chow father and 13.23% from high-Hcy chow father, and the difference of absorption rate was statistically significant ($p = 0.0178$, RR = 9.4, 95%CI = 1.61–56.68, Figure 3A). Then, we observed the development of the fetus mice heart. To eliminate the experiment bias of gestation relative disease, like gestational diabetes, the physiologic index of pregnant mouse was monitored during gestation, and cardiac phenotypes of the embryos in E14.5 were examined via histological analysis. Results revealed that although food intake, body weight, blood pressure, pulse, and blood glucose levels in pregnant mice were not affected (Figure 3B), we found only one type of heart defect in our study——perimembranous ventricular septal defect, and the incidence of ventricular septal defect in embryos from high-Hcy fathers significantly increased (Figure 3C). The proportion of pregnant mice with VSD offspring was 37.5% (3 in 8) and 100% (8 in 8) in the paternal control and high-Hcy groups, respectively (Figure 3D). VSD occurrence for all the offspring was 4.29% in the control group (3 in 70) and 28.81% (17 in 59) in paternal high-Hcy group ($p = 0.0001$, RR = 6.72, 95%CI = 2.07–21.83, Figure 3E). These results indicated paternal high Hcy levels increased risk for CHD in offspring.

Genome DNA methylation analyses identified differential methylation in sperm DNA

Decreased sperm counts and sperm motility defects were not directly associated with the risk of CHD in offspring. To explore the mechanism of paternal hyperhomocysteinemia-caused CHD in the F1 mice, we firstly checked sperm histone H3K4, H3K27, and H3K36 methylation, which are the few histone modifications after protamines replacement. Western blotting revealed no significant difference in the levels of histone H3 methylation at K4, K27, and K36 in epididymal sperm extracts between high-Hcy and control mice (Figure 4A). Secondly, whole sperm genome DNA methylation was performed and the data analyses showed that paternal high-Hcy caused significant changes in DNA methylation levels in CHD-related genes in sperm (Figure 4B). Among those differentially methylated regions, we found significant changes in DNA methylation levels in the promoter regions of CHD-related genes, such as *Nfatc1* and *Acvr1*, which are implicated in heart development and

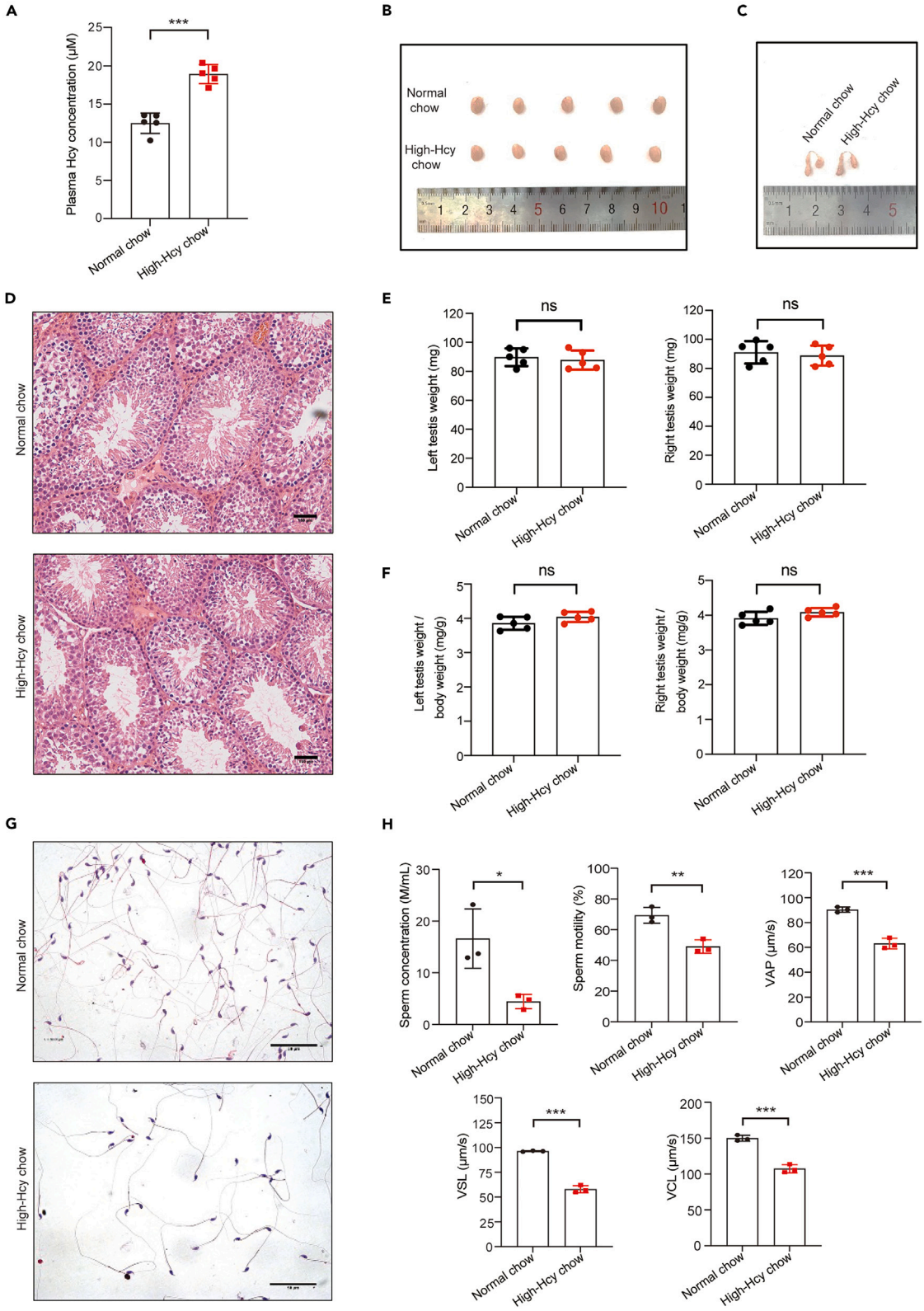
A
Plasma Hcy concentration (μM)
***
Normal chow
High-Hcy chow
B
Normal chow
High-Hcy chow
C
Normal chow
High-Hcy chow
D
Normal chow
High-Hcy chow
E
Left testis weight (mg)
ns
Right testis weight (mg)
ns
F
Left testis weight / body weight (mg/g)
ns
Right testis weight / body weight (mg/g)
ns
G
Normal chow
High-Hcy chow
H
Sperm concentration (M/mL)
*
Sperm motility (%)
**
VAP (μm/s)
***
VSL (μm/s)
***
VCL (μm/s)
***

Figure 2. Paternal high Hcy caused abnormal sperm count and motility

(A) Hcy levels in male mouse given high-Hcy water or not.

(B and C) The size of left testis and epididymis in normal chow or high-Hcy chow male mouse.

(D) Assessment of spermatogenesis in adult control and HHcy mice. Testes were fixed overnight in Bouin's fluid, dehydrated in ethanol, and embedded in paraffin. Tissue sections (6 μm) were stained with HE and examined under a light microscope. Scale bars = 100 μm.

(E and F) Testis weight and testis body weight ratio of normal and high-Hcy chow male mouse.

(G) Morphology of epididymal sperm from control and High-Hcy mice. Scale bars = 50 μm.

(H) Computer-assisted sperm analyses of epididymal sperm collected from adult control and High-Hcy male mice. Parameters analyzed included sperm count, total motility, average path velocity (VAP), straight line velocity (VSL), and curvilinear velocity (VCL).

correlated with VSD phenotypes (Figure 4C).[23] Moreover, we compared those CHD-related genes RNA expressions of paternal sperms and offspring's embryo heart tissues in two group and found homocysteine indeed changed *Robo1*, *Nfatc1*, *Acvr1*, and *Meis2* RNA expression level in two generations (Figures 4D and 4E). Further, western blotting showed a significant decrease in expression of DNA methyltransferases DNMT3A and DNMT3B in sperm from high-Hcy mice, compared to controls (Figure 4A), suggesting that Hcy might affect DNA methylation by altering DNMT expression.

Folic acid could rescue paternal HHcy-caused ventricular septal defect

To rescue the teratogenic effect of paternal high-Hcy. Male mice with high-Hcy levels were given 10 mg folic acid per kilogram chow (10FS) and 20 mg folic acid per kilogram chow (20FS). Plasma Hcy concentration was detected among the groups. The results showed that 20 mg folic acid per kilogram chow supplement could reduce high-Hcy chow-induced high plasma Hcy concentration to near normal concentration. (Figure 5A), 20FS diet was used to carry out follow-up experiments and we found that folic acid significantly decreased incidence of VSD in offspring in high-Hcy male mice (Figure 5B) and incidence of embryo absorption induced by high-Hcy (17.8% vs. 4.54%) (Figure 5C). Moreover, there was significant decrease in the percentages of pregnant mice bearing VSD offspring (Figure 5B) and the incidence of VSD in embryos (24.32%–4.76%) (Figure 5D). These results further demonstrated that increased paternal Hcy levels caused elevated risk for CHD in offspring.

DISCUSSION

In the present study, we examined whether childbearing male mice with high Hcy caused abnormal spermatogenesis and had a harmful effect on embryo or infant development particularly in heart. We found decreased sperm counts and impaired sperm motility in high Hcy male mice. Meanwhile, we also found embryo miscarriage and heart malformation in F1 offspring of high Hcy father. The heart influence of high Hcy male mice on offspring was associated with altered promoter methylation of the CHD-related gene, including *Nfatc1*, *Robo1*, *Acvr1*, and *Meis2*. Moreover, the teratogenic effect of paternal Hcy could be rescued by folic acid supplement before mating.

NFATc1 is a transcriptional regulator of endothelial cell fate, and is considered as an essential role for cardiac cushion formation.[24–26] In mice model, it is reported that *Nfatc* knock out embryo displays conspicuous pulmonary and the aortic valves leaflets absence and ventricular septal defect.[27,28] ROBO1 is receptor of Slit-Robo signaling which functions in a variety of developmental processes.[29] Multiple types of congenital heart disease (CHD) were identified in human and mouse *Robo1* mutants.[30] Moreover, ventricular septal defect is one of the most common type.[31,32] In regard to *Meis2*, recent study has identified it as a gene essential for cranial and cardiac neural crest development.[33] VSD was reported as a common phenotype of patients carrying *MEIS2* mutation.[34] Ventricular septal defect was the only type of cardiac defect found in our study, cardiac defect phenotype is accordance with the mutation genes, like *Nfatc1*, *Robo1*, and *Meis2*. However, the common cardiac phenotype of *Acvr1* mutation was atrioventricular septum defects (AVSD).[35] We speculate the reason why the AVSD was not observed in this study was that the sample number of F1 offspring was not enough.

The mechanism between elevated maternal Hcy and increased risk of CHD in offspring is controversial. Numerous experimental studies have shown that through directly generating reactive oxygen species[36] or inhibiting antioxidant system,[37] Hcy induces cellular and molecular oxidative injury, which is past referred as the key pathogenic mechanism in cardiovascular disease. However, recent study has found that hyperhomocysteinemia plays a pathogenic role by inducing its target protein, like superoxide dismutases (SOD1/2) lysine-N-homocysteinylation.[38] Moreover, there are some evidences showing that Hcy impairs epigenetic control of gene expression mediated by DNA methylation, histone modifications, and non-coding RNA, which was the pathology of disease, including cardiovascular and cerebrovascular disease.[39] In a high-Met diet *ApoE*$^{-/-}$ mice, high Hcy could upregulate expression of miR-149a/152, and decrease DNMT1 mRNA and protein levels in the aorta, which is associated with atherosclerosis.[40] And in high Hcy genetic model (male mice Tg-128T *Cbs*$^{-/-}$), high Hcy reduces expression of DNMT1, DNMT3A and DNMT3B and methylation of *5LO* DNA, thereby contributing to up-regulation of 5LO mRNA and protein and β-amyloid formation, which may be pathogenesis of Alzheimer's disease.[41] In our study, we observed that high Hcy reduced expression of DNMT3A and DNMT3B and methylation changes of several CHD-related genes. We speculate decreased DNMT3A and DNMT3B participate in the mechanism of changes of CHD-related gene methylation level. Because we only observed the decreased expression of DNMT3A and DNMT3B, whether other DNA methyltransferases participated in or not remained unknown. Further analysis on will be required for clarifying the molecular role of Hcy-induced DNA methylation alternations in intergenerational inheritance.

Folic acid fortification has been recommended for reproductive-age woman by the US Public Health Service since 1992. And this action reduces the prevalence of neural tube malformation by 19% decline in nearly 10 years.[42] And recent studies based on a large sample have shown that food fortification with folic acid have a benefit of a reduction in the birth prevalence of specific CHD.[43,44] Aside from this, paternal

A

Incidence of embryos absorption

	Total births	Absorbed fetuses	Total live births	Absorption rate	P value	RR(95%)
Normal chow	71	1	70	1.41%	—	—
High-Hcy chow	68	9	59	13.23%	0.0178	9.40 (1.61-56.68)

B

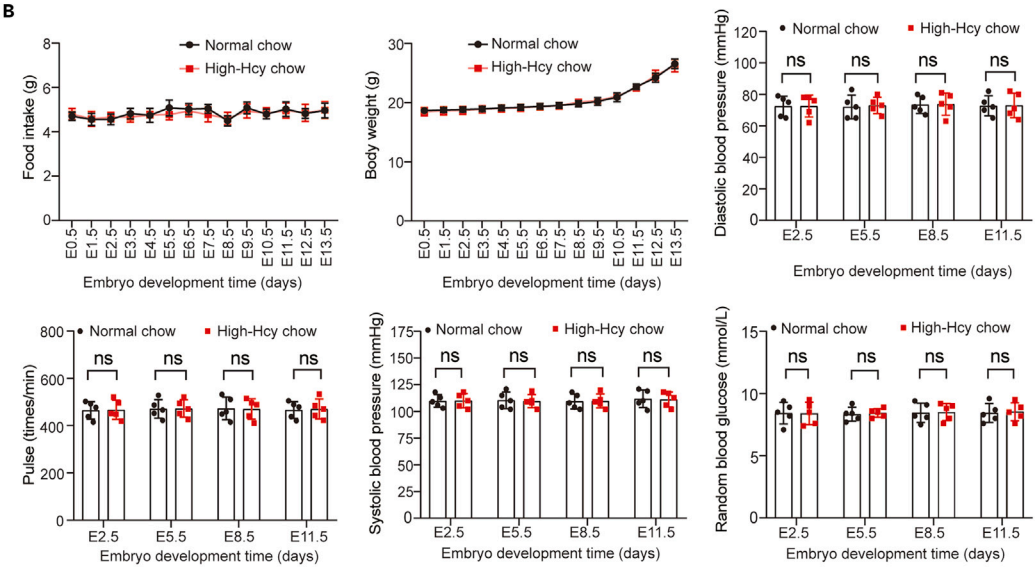

C

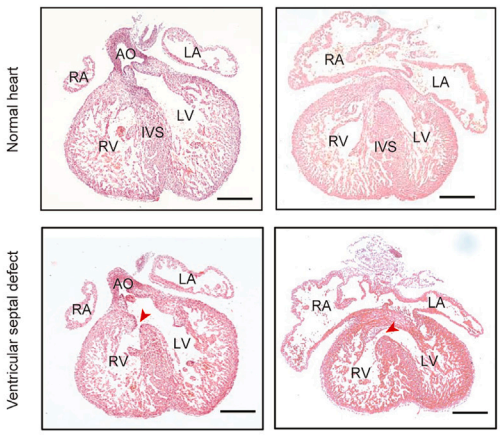

D

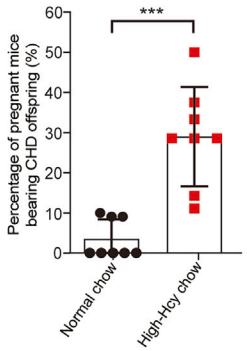

E

Incidence of CHD embryos

	Pregnant mice	Total live births	Normal	VSD	Ratio of VSD	P value	RR(95%)
Normal chow	8	70	67	3	4.29%	—	—
High-Hcy chow	8	59	42	17	28.81%	0.0001	6.72 (2.07-21.83)

Figure 3. Paternal high Hcy contributed to congenital heart disease

(A) Incidence of embryos absorption obtained from paternal mice fed with either high-Hcy chow or normal chow.

(B) Physiologic index of pregnant mice.

(C) Confirmation of heart structure by hematoxylin eosin (HE) staining. RA, right atrium; RV, right ventricle; LA, left atrium; LV, left ventricle; AO, aorta; IVS, intact ventricular septum, arrowhead indicated ventricular septal defect bar = 50 μm.

(D) Proportion of CHD offspring obtained from male mice fed with either high-Hcy chow or normal chow, unpaired *t* test with Welch's correction, p = 0.0004.

(E) Incidence of CHD embryos in pregnant mice mated with male mice fed with either high-Hcy or normal chow. [§]Chi-square test.

folate deficiency has been found to alter the sperm epigenome and is associated with the risk of craniofacial and musculoskeletal malformations.[45,46] Since we previously found that folate deficiency induced CHD through increasing Hcy signals,[38,47] therefore, our findings indicate that high-Hcy-induced epigenetic changes in sperm increased the risk of CHD in offspring.

Limitations of the study

This study was mainly performed in mouse model, and more clinical samples are needed to verify the results in the future. In addition, although we show that homocysteine reduces DNMT3A/3B in sperm, we have not determined the detailed molecular mechanism.

STAR★METHODS

Detailed methods are provided in the online version of this paper and include the following:

- KEY RESOURCES TABLE
- RESOURCE AVAILABILITY
  - Lead contact
  - Materials availability
  - Data and code availability
- EXPERIMENTAL MODEL AND STUDY PARTICIPANT DETAILS
  - Mice model
- METHOD DETAILS
  - Hcy quantification
  - Assessment of food intake, weight, blood pressure, pulse, and blood glucose levels of pregnant mice
  - Mouse embryo heart isolation and histological analysis
  - Sperm preparation
  - Computer-assisted sperm analysis
  - Western blotting
  - Reverse transcipition and quantitative reverse transcription-PCR (qRT-PCR)
  - Testis and sperm histology
  - Whole-genome bisulfite sequencing (WGBS) mapping and relative analysis
- QUANTIFICATION AND STATISTICAL ANALYSIS

SUPPLEMENTAL INFORMATION

Supplemental information can be found online at https://doi.org/10.1016/j.isci.2024.109447.

ACKNOWLEDGMENTS

This work was supported by the Grants from Key Development Programs of Basic Research of China (Nos. 2019YFA0801900 and 2020YFA0803601), China Postdoctoral Science Foundation (No. 2022M710774), National Natural Science Foundation of China (Nos. 82330048, 31871432 and 81771627), Shanghai Outstanding Academic Leaders Program (No. 21XD1421700), and the Innovation Program of the Shanghai Municipal Education Commission (No. 2023ZKZD24).

AUTHOR CONTRIBUTIONS

The author contribution is as follows: J.Y.Z. conceived the study; J.Y.Z. and Y.H.G. designed and supervised the experiments; L.L., X.Z., H.R.G., and Y.N.Q. performed the experiments and analyzed the data; L.L., X.Z., and H.R.G. generated the animal models; All authors read and discussed the manuscript.

DECLARATION OF INTERESTS

The authors declare no competing interests.

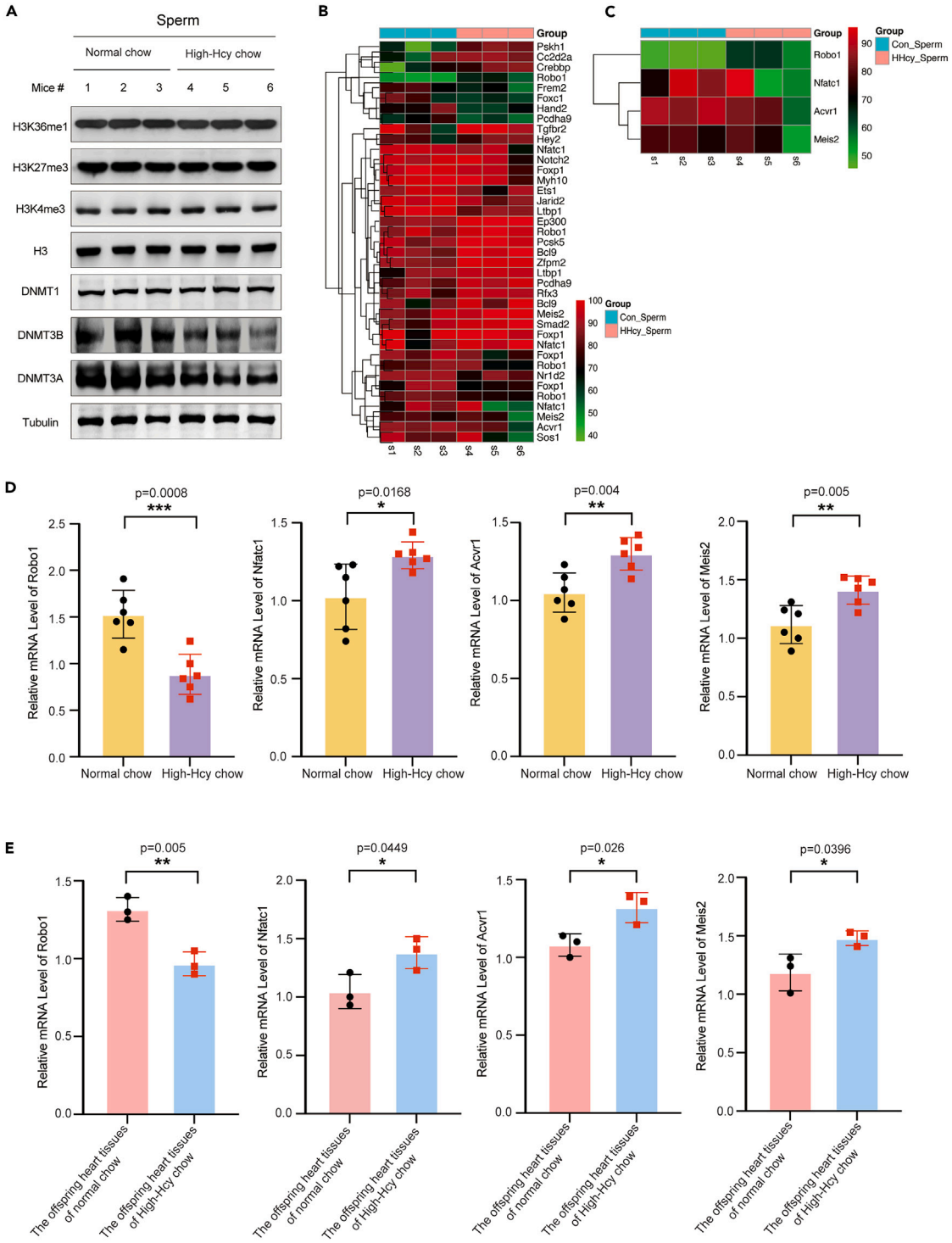

Figure 4. Hcy changed CHD-related genes methylation of sperm genome

(A) Western blot analyses for levels of histone methylation and DNA transferases in sperm.

(B) Heat maps showing the difference of various differentially methylated regions in CHD-related genes in male mice sperms.

(C) Heat maps showing the significant changes in DNA methylation levels in the promoter regions of CHD-related genes.

(D) The mRNA expression of *Robo1*, *Nfatc1*, *Acvr1*, and *Meis2* in sperms of two group.

Unpaired *t* test.

(E) The mRNA expression of *Robo1*, *Nfatc1*, *Acvr1*, and *Meis2* in all live-birth embryo heart tissues of every female mated with normal chow or high-Hcy chow male mice. Unpaired *t* test.

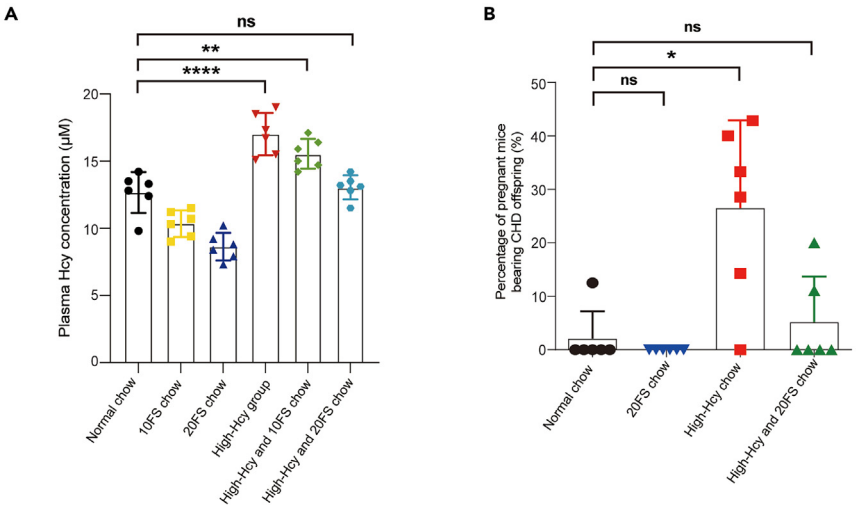

C

Incidence of embryo absorption

	Total births	Absorbed fetuses	Total live births	Absorption rate	P value	RR(95%)
Normal chow	45	1	44	2.22%	——	——
20FS chow	43	2	40	4.76%	0.95[a]	——
High-Hcy chow	45	8	37	17.8%	0.035[a]	1.19 (1.04-1.43)
High-Hcy + 20FS chow	44	2	42	4.54%	0.98[a]	2.10(0.24-31.0)

D

Incidence of CHD embryos

	Pregnant mice	Total live births	Normal	VSD	Ratio of VSD	P value	RR(95%)
Normal chow	6	44	43	1	2.27%	——	——
20FS chow	6	40	40	0	0%	1.00[a]	——
High-Hcy chow	6	37	28	9	24.32%	0.0077[b]	10.70 (1.42-80.66)
High-Hcy + 20 FS chow	6	42	40	2	4.76%	0.97[b]	2.10(0.20-22.27)

Figure 5. Folic acid rescue paternal high Hcy-caused congenital heart disease

(A) Plasma Hcy levels of different groups in mouse.

(B) Proportion of CHD offspring obtained from pregnant mice mated with male mice fed with different diets used in this study.

(C) Incidence of embryo absorption in pregnant mice mated with male mice fed with different diets , [a]Chi-square with Yates' correction.

(D) Incidence of embryos with CHD in pregnant mice mated with male mice fed with different diets, [a]Fisher's exact test, [b]Chi-square with Yates' correction.

Received: September 10, 2023
Revised: January 18, 2024
Accepted: March 5, 2024
Published: March 7, 2024

REFERENCES

1. Ng, S.F., Lin, R.C.Y., Laybutt, D.R., Barres, R., Owens, J.A., and Morris, M.J. (2010). Chronic high-fat diet in fathers programs beta-cell dysfunction in female rat offspring. Nature *467*, 963–966. https://doi.org/10.1038/nature09491.
2. Mejia-Lancheros, C., Mehegan, J., Murrin, C.M., and Kelleher, C.C.; Lifeways Cross-Generation Cohort Study Group (2018). Smoking habit from the paternal line and grand-child's overweight or obesity status in early childhood: prospective findings from the lifeways cross-generation cohort study. Int. J. Obes. *42*, 1853–1870. https://doi.org/10.1038/s41366-018-0039-8.
3. Yang, F., Yuan, W., Liang, H., Song, X., Yu, Y., Gelaye, B., Miao, M., and Li, J. (2019). Preconceptional paternal antiepileptic drugs use and risk of congenital anomalies in offspring: a nationwide cohort study. Eur. J. Epidemiol. *34*, 651–660. https://doi.org/10.1007/s10654-019-00509-2.
4. Gong, Y., Xue, Y., Li, X., Zhang, Z., Zhou, W., Marcolongo, P., Benedetti, A., Mao, S., Han, L., Ding, G., and Sun, Z. (2021). Inter- and Transgenerational Effects of Paternal Exposure to Inorganic Arsenic. Adv. Sci. *8*, 2002715. https://doi.org/10.1002/advs.202002715.
5. Ryan, D.P., Henzel, K.S., Pearson, B.L., Siwek, M.E., Papazoglou, A., Guo, L., Paesler, K., Yu, M., Müller, R., Xie, K., et al. (2018). A paternal methyl donor-rich diet altered cognitive and neural functions in offspring mice. Mol. Psychiatr. *23*, 1345–1355. https://doi.org/10.1038/mp.2017.53.
6. Åsenius, F., Danson, A.F., and Marzi, S.J. (2020). DNA methylation in human sperm: a systematic review. Hum. Reprod. Update *26*, 841–873. https://doi.org/10.1093/humupd/dmaa025.
7. Schagdarsurengin, U., Paradowska, A., and Steger, K. (2012). Analysing the sperm epigenome: roles in early embryogenesis and assisted reproduction. Nat. Rev. Urol. *9*, 609–619. https://doi.org/10.1038/nrurol.2012.183.
8. Gapp, K., van Steenwyk, G., Germain, P.L., Matsushima, W., Rudolph, K.L.M., Manuella, F., Roszkowski, M., Vernaz, G., Ghosh, T., Pelczar, P., et al. (2020). Alterations in sperm long RNA contribute to the epigenetic inheritance of the effects of postnatal trauma. Mol. Psychiatr. *25*, 2162–2174. https://doi.org/10.1038/s41380-018-0271-6.
9. Oliva, R., and Dixon, G.H. (1991). Vertebrate protamine genes and the histone-to-protamine replacement reaction. Prog. Nucleic Acid Res. Mol. Biol. *40*, 25–94. https://doi.org/10.1016/s0079-6603(08)60839-9.
10. Steger, K. (1999). Transcriptional and translational regulation of gene expression in haploid spermatids. Anat. Embryol. *199*, 471–487. https://doi.org/10.1007/s004290050245.
11. Zhang, W., Yang, J., Lv, Y., Li, S., and Qiang, M. (2019). Paternal benzo[a]pyrene exposure alters the sperm DNA methylation levels of imprinting genes in F0 generation mice and their unexposed F1-2 male offspring. Chemosphere *228*, 586–594. https://doi.org/10.1016/j.chemosphere.2019.04.092.
12. McCarthy, D.M., Morgan, T.J., Jr., Lowe, S.E., Williamson, M.J., Spencer, T.J., Biederman, J., and Bhide, P.G. (2018). Nicotine exposure of male mice produces behavioral impairment in multiple generations of descendants. PLoS Biol. *16*, e2006497. https://doi.org/10.1371/journal.pbio.2006497.
13. Liao, D., Yang, X., and Wang, H. (2007). Hyperhomocysteinemia and high-density lipoprotein metabolism in cardiovascular disease. Clin. Chem. Lab. Med. *45*, 1652–1659. https://doi.org/10.1515/CCLM.2007.358.
14. Pang, H., Han, B., Fu, Q., and Zong, Z. (2016). Association of High Homocysteine Levels With the Risk Stratification in Hypertensive Patients at Risk of Stroke. Clin. Therapeut. *38*, 1184–1192. https://doi.org/10.1016/j.clinthera.2016.03.007.
15. Mills, J.L., McPartlin, J.M., Kirke, P.N., Lee, Y.J., Conley, M.R., Weir, D.G., and Scott, J.M. (1995). Homocysteine metabolism in pregnancies complicated by neural-tube defects. Lancet *345*, 149–151. https://doi.org/10.1016/s0140-6736(95)90165-5.
16. Hobbs, C.A., Cleves, M.A., Melnyk, S., Zhao, W., and James, S.J. (2005). Congenital heart defects and abnormal maternal biomarkers of methionine and homocysteine metabolism. Am. J. Clin. Nutr. *81*, 147–153. https://doi.org/10.1093/ajcn/81.1.147.
17. Yadav, U., Kumar, P., and Rai, V. (2021). Maternal biomarkers for early prediction of the neural tube defects pregnancies. Birth Defects Res. *113*, 589–600. https://doi.org/10.1002/bdr2.1842.
18. Rosenquist, T.H., Ratashak, S.A., and Selhub, J. (1996). Homocysteine induces congenital defects of the heart and neural tube: effect of folic acid. Proc. Natl. Acad. Sci. USA *93*, 15227–15232. https://doi.org/10.1073/pnas.93.26.15227.
19. Yang, B., Fan, S., Zhi, X., Wang, Y., Wang, Y., Zheng, Q., and Sun, G. (2014). Prevalence of hyperhomocysteinemia in China: a systematic review and meta-analysis. Nutrients *7*, 74–90. https://doi.org/10.3390/nu7010074.
20. Challa, F., Getahun, T., Sileshi, M., Nigassie, B., Geto, Z., Ashibire, G., Gelibo, T., Teferra, S., Seifu, D., Sitotaw, Y., et al. (2020). Prevalence of Hyperhomocysteinaemia and Associated Factors among Ethiopian Adult Population in a 2015 National Survey. BioMed Res. Int. *2020*, 9210261. https://doi.org/10.1155/2020/9210261.
21. Zhang, X., Qu, Y.Y., Liu, L., Qiao, Y.N., Geng, H.R., Lin, Y., Xu, W., Cao, J., and Zhao, J.Y. (2021). Homocysteine inhibits pro-insulin receptor cleavage and causes insulin resistance via protein cysteine-homocysteinylation. Cell Rep. *37*, 109821. https://doi.org/10.1016/j.celrep.2021.109821.
22. Castillo, J., Jodar, M., and Oliva, R. (2018). The contribution of human sperm proteins to the development and epigenome of the preimplantation embryo. Hum. Reprod. Update *24*, 535–555. https://doi.org/10.1093/humupd/dmy017.
23. Williams, K., Carson, J., and Lo, C. (2019). Genetics of Congenital Heart Disease. Biomolecules *9*, 879. https://doi.org/10.3390/biom9120879.
24. Armstrong, E.J., and Bischoff, J. (2004). Heart valve development: endothelial cell signaling and differentiation. Circ. Res. *95*, 459–470. https://doi.org/10.1161/01.RES.0000141146.95728.da.
25. Combs, M.D., and Yutzey, K.E. (2009). VEGF and RANKL regulation of NFATc1 in heart valve development. Circ. Res. *105*, 565–574. https://doi.org/10.1161/CIRCRESAHA.109.196469.
26. Wu, B., Wang, Y., Lui, W., Langworthy, M., Tompkins, K.L., Hatzopoulos, A.K., Baldwin, H.S., and Zhou, B. (2011). Nfatc1 coordinates valve endocardial cell lineage development required for heart valve formation. Circ. Res. *109*, 183–192. https://doi.org/10.1161/CIRCRESAHA.111.245035.
27. Ranger, A.M., Grusby, M.J., Hodge, M.R., Gravallese, E.M., de la Brousse, F.C., Hoey, T., Mickanin, C., Baldwin, H.S., and Glimcher, L.H. (1998). The transcription factor NF-ATc is essential for cardiac valve formation. Nature *392*, 186–190. https://doi.org/10.1038/32426.
28. de la Pompa, J.L., Timmerman, L.A., Takimoto, H., Yoshida, H., Elia, A.J., Samper, E., Potter, J., Wakeham, A., Marengere, L., Langille, B.L., et al. (1998). Role of the NF-ATc transcription factor in morphogenesis of cardiac valves and septum. Nature *392*, 182–186. https://doi.org/10.1038/32419.
29. Blockus, H., and Chédotal, A. (2016). Slit-Robo signaling. Development *143*, 3037–3044. https://doi.org/10.1242/dev.132829.
30. Zhao, J., and Mommersteeg, M.T.M. (2018). Slit-Robo signalling in heart development. Cardiovasc. Res. *114*, 794–804. https://doi.org/10.1093/cvr/cvy061.
31. Mommersteeg, M.T.M., Yeh, M.L., Parnavelas, J.G., and Andrews, W.D. (2015). Disrupted Slit-Robo signalling results in membranous ventricular septum defects and bicuspid aortic valves. Cardiovasc. Res. *106*, 55–66. https://doi.org/10.1093/cvr/cvv040.
32. Kruszka, P., Tanpaiboon, P., Neas, K., Crosby, K., Berger, S.I., Martinez, A.F., Addissie, Y.A., Pongprot, Y., Sittiwangkul, R., Silvilairat, S., et al. (2017). Loss of function in ROBO1 is associated with tetralogy of Fallot and septal defects. J. Med. Genet. *54*, 825–829. https://doi.org/10.1136/jmedgenet-2017-104611.
33. Machon, O., Masek, J., Machonova, O., Krauss, S., and Kozmik, Z. (2015). Meis2 is essential for cranial and cardiac neural crest development. BMC Dev. Biol. *15*, 40. https://doi.org/10.1186/s12861-015-0093-6.
34. Giliberti, A., Currò, A., Papa, F.T., Frullanti, E., Ariani, F., Coriolani, G., Grosso, S., Renieri, A., and Mari, F. (2020). MEIS2 gene is responsible for intellectual disability, cardiac defects and a distinct facial phenotype. Eur. J. Med. Genet. *63*, 103627. https://doi.org/10.1016/j.ejmg.2019.01.017.
35. Valer, J.A., Sanchez-de-Diego, C., Pimenta-Lopes, C., Rosa, J.L., and Ventura, F. (2019). ACVR1 Function in Health and Disease. Cells *8*, 1366. https://doi.org/10.3390/cells8111366.
36. Chang, L., Xu, J., Yu, F., Zhao, J., Tang, X., and Tang, C. (2004). Taurine protected myocardial mitochondria injury induced by hyperhomocysteinemia in rats. Amino Acids *27*, 37–48. https://doi.org/10.1007/s00726-004-0096-2.
37. Wu, B., Yue, H., Zhou, G.H., Zhu, Y.Y., Wu, T.H., Wen, J.F., Cho, K.W., and Jin, S.N. (2019). Protective effects of oxymatrine on homocysteine-induced endothelial injury: Involvement of mitochondria-dependent apoptosis and Akt-eNOS-NO signaling pathways. Eur. J. Pharmacol. *864*, 172717. https://doi.org/10.1016/j.ejphar.2019.172717.
38. Mei, X., Qi, D., Zhang, T., Zhao, Y., Jin, L., Hou, J., Wang, J., Lin, Y., Xue, Y., Zhu, P., et al.

(2020). Inhibiting MARSs reduces hyperhomocysteinemia-associated neural tube and congenital heart defects. EMBO Mol. Med. *12*, e9469. https://doi.org/10.15252/emmm.201809469.

39. Perła-Kaján, J., and Jakubowski, H. (2019). Dysregulation of Epigenetic Mechanisms of Gene Expression in the Pathologies of Hyperhomocysteinemia. Int. J. Mol. Sci. *20*, 3140. https://doi.org/10.3390/ijms20133140.
40. Yang, A., Sun, Y., Gao, Y., Yang, S., Mao, C., Ding, N., Deng, M., Wang, Y., Yang, X., Jia, Y., et al. (2017). Reciprocal Regulation Between miR-148a/152 and DNA Methyltransferase 1 Is Associated with Hyperhomocysteinemia-Accelerated Atherosclerosis. DNA Cell Biol. *36*, 462–474. https://doi.org/10.1089/dna.2017.3651.
41. Li, J.G., Barrero, C., Gupta, S., Kruger, W.D., Merali, S., and Praticò, D. (2017). Homocysteine modulates 5-lipoxygenase expression level via DNA methylation. Aging Cell *16*, 273–280. https://doi.org/10.1111/acel.12550.
42. Honein, M.A., Paulozzi, L.J., Mathews, T.J., Erickson, J.D., and Wong, L.Y. (2001). Impact of folic acid fortification of the US food supply on the occurrence of neural tube defects. JAMA *285*, 2981–2986. https://doi.org/10.1001/jama.285.23.2981.
43. Liu, S., Joseph, K.S., Luo, W., León, J.A., Lisonkova, S., Van den Hof, M., Evans, J., Lim, K., Little, J., Sauve, R., et al. (2016). Effect of Folic Acid Food Fortification in Canada on Congenital Heart Disease Subtypes. Circulation *134*, 647–655. https://doi.org/10.1161/CIRCULATIONAHA.116.022126.
44. Qu, Y., Lin, S., Zhuang, J., Bloom, M.S., Smith, M., Nie, Z., Mai, J., Ou, Y., Wu, Y., Gao, X., et al. (2020). First-Trimester Maternal Folic Acid Supplementation Reduced Risks of Severe and Most Congenital Heart Diseases in Offspring: A Large Case-Control Study. J. Am. Heart Assoc. *9*, e015652. https://doi.org/10.1161/JAHA.119.015652.
45. Lismer, A., Dumeaux, V., Lafleur, C., Lambrot, R., Brind'Amour, J., Lorincz, M.C., and Kimmins, S. (2021). Histone H3 lysine 4 trimethylation in sperm is transmitted to the embryo and associated with diet-induced phenotypes in the offspring. Dev. Cell *56*, 671–686.e6. https://doi.org/10.1016/j.devcel.2021.01.014.
46. Lambrot, R., Xu, C., Saint-Phar, S., Chountalos, G., Cohen, T., Paquet, M., Suderman, M., Hallett, M., and Kimmins, S. (2013). Low paternal dietary folate alters the mouse sperm epigenome and is associated with negative pregnancy outcomes. Nat. Commun. *4*, 2889. https://doi.org/10.1038/ncomms3889.
47. Wang, D., Wang, F., Shi, K.H., Tao, H., Li, Y., Zhao, R., Lu, H., Duan, W., Qiao, B., Zhao, S.M., et al. (2017). Lower Circulating Folate Induced by a Fidgetin Intronic Variant Is Associated With Reduced Congenital Heart Disease Susceptibility. Circulation *135*, 1733–1748. https://doi.org/10.1161/CIRCULATIONAHA.116.025164.

STAR★METHODS

KEY RESOURCES TABLE

REAGENT or RESOURCE	SOURCE	IDENTIFIER
Antibodies		
H3K36me1	Abcam	Cat#ab9048
H3K27me3	Cell Signaling Technology	Cat#9756
H3K4me3	Cell Signaling Technology	Cat#9751
H3	Abmart	Cat#P30266
DNMT1	Abcam	Cat#ab188453
DNMT3B	Cell Signaling Technology	Cat#67259
DNMT3A	Abcam	Cat#ab307503
Tubulin	GenScript	Cat#A01410
anti-mouse secondary antibodies	GenScript	Cat#A00160
anti-rabbit secondary antibodies	GenScript	Cat#A00098
Chemicals, peptides, and recombinant proteins		
Bouin's Fluid	G-CLONE	Cat# RS4141
4% paraformaldehyde	Servicebio	Cat# G1101
Hematoxylin-Eosin staining Kit	Sangon Biotech	Cat# E607318
Critical commercial assays		
homocysteine ELISA kit	Kanglang Biotech	Cat#KL-Hcy-Mu
HiScript III 1st strand cDNA Synthesis Kit	Vazyme	Cat# R312-02
ChamQ SYBR qRCR Master Mix	Vazyme	Cat# Q321-02
Experimental models: Organisms/strains		
C57BL/6J	Beijing Vital River Laboratory Animal Technology Co. Ltd	N/A
Oligonucleotides		
Oligonucleotides are listed in Table S1	This study	N/A
Software and algorithms		
ImageJ	NIH	https://imagej.nih.gov/ij/
GraphPad Prim9	GraphPad Software	https://www.graphpad.com/features

RESOURCE AVAILABILITY

Lead contact

Further information and requests for resources and reagents should be directed to and will be fulfilled by the lead contact, Jian-Yuan Zhao (zhaojy@vip.163.com).

Materials availability

This study did not generate new unique reagents.

Data and code availability

- Data reported in this paper will be shared by the lead contact upon request.
- This paper does not report original code.
- Any additional information required to reanalyze the data reported in this paper is available from the lead contact upon request.

EXPERIMENTAL MODEL AND STUDY PARTICIPANT DETAILS

Mice model

Four-week-old male C57BL/6J mice were obtained from Vital River (Beijing). The mice were fed a standard diet and had free access to water. During the experiment, the mice were housed in cages in a light-, temperature- and humidity-controlled environment. Normal chow group was fed a standard AIN-93G diet (containing 2mg folic acid per chow), folate acid supplemented group included 10mg folic acid per kilogram chow (10FS) and 20mg folic acid per kilogram chow (20FS). High-Hcy chow was fed 2 g/L Hcy in water for 9–11 weeks. Then, we measured the plasma Hcy concentration in mice of each group. In the meantime, C57BL/6J female mice, mostly born from the same parents, was assigned each group randomly and equally to make sure the same genetic background. Then, male mice were mated with female mice with normal feeding. After mating, the pregnant mice were kept in the same environment without any drug intervention, and the physiologic index of the mice was monitored during pregnancy. The cardiac phenotypes of the embryos in E14.5 were examined via histological analysis. All animal experiments were approved by the Fudan University Animal Care and Use Committee and were conducted in accordance with the National Institutes of Health Guidelines for the Care and Use of Laboratory Animals.

METHOD DETAILS

Hcy quantification

To obtain plasma from mice, one eyeball from each animal was ejected with scissors and completely removed. Blood from the retroorbital plexus was collected in EDTA-coated 1.5 mL tubes and centrifuged immediately. Then, the plasma samples were collected and stored at −80°C until determination of Hcy content using a homocysteine ELISA kit (Kanglang Biotech).

Assessment of food intake, weight, blood pressure, pulse, and blood glucose levels of pregnant mice

Pregnant mice were housed individually in cages. The food intake and weight of each pregnant mouse was recorded daily at 9 a.m. from E0.5 to E13.5. Blood pressure, pulse, and random blood glucose levels of each pregnant mouse were assessed simultaneously every 3 days during E0.5 to E13.5 using a non-invasive animal blood-pressure meter (Visitech Systems, BP-2000, Visitech Systems, Apex, New York, USA) and glucose meter (Roche, Accu-chek, Roche, Basel, Switzerland). The fasting blood glucose of each pregnant mouse was assessed at E14.5.

Mouse embryo heart isolation and histological analysis

E14.5 embryonic hearts were dissected and fixed in 4% paraformaldehyde. The hearts were dehydrated using graded ethanol series, followed by vitrification using dimethylbenzene. Consequently, the heart tissues were embedded in paraffin and sectioned from the beginning to end tissue in a coronal plane with the thickness of 5 μm. All sections were then deparaffinized, rehydrated in graded alcohol series, and stained with hematoxylin-eosin. Every stained slice of the heart tissue was observed to determine whether there are malformation of the heart using a Nikon microscope (Ni-U, Nikon, Minato-ku, Japan) and analyzed using ImageJ software. For septal defect type of CHD, it was determined when a defect was present in a setion accompanied by the same site defect in several consecutive sections.

Sperm preparation

The cauda epididymis was dissected and obtained from euthanized mice. Next, the tissues were cut into small pieces and incubated in 500 μL of PBS solution at 37°C for 30 min to free sperm from the epididymis.

Computer-assisted sperm analysis

First, the sperm suspension was diluted to an appropriate concentration and loaded on to a chamber slide. Sperm parameters, including sperm concentration, total motility, average path velocity, progressive velocity, and curvilinear velocity, were analyzed using a computer-assisted sperm analysis (CASA) system.

Western blotting

Sperm was resuspended in sperm lysis buffer (PBS containing 0.5% SDS, 10 mM DTT, 5 mM EDTA, protease inhibitors) and incubated at 37°C for 30 min. After sonication to shear genomic DNA, samples were prepared by adding 5 × SDS sample loading buffer to each lysate. After centrifugation at 16,000 × g and 4°C for 15 min, the lysate supernatants were analyzed via western blotting according to standard procedures. Protein expression was detected by measuring chemiluminescence on a Typhoon FLA9500 (GE Healthcare, Little Chalfont, UK).

Reverse transcipition and quantitative reverse transcription-PCR (qRT-PCR)

Total RNA was obtained from Sperm or embryo heart tissue by Trizol reagents after tissue grinding and converted into cDNA using the Hi-Script III 1st strand cDNA Synthesis Kit (Vazyme, Nanjing, China). The mRNA levels of *Robo1*, *Nfatc1*, *Acvr1*, and *Meis2* were determined by using qRT-PCR with the CFX96 Touch real-time PCR detection system (Bio-Rad, Hercules, USA). β-actin was used as the internal reference gene. Each reation was performed three times. All primers used in the experiment are listed in the Table S1.

Testis and sperm histology

For histological studies, the testis was fixed overnight in Bouin's fluid, dehydrated in ethanol, and embedded in paraffin. Tissue sections were mounted on glass slides and dried at 65°C for 7 h. The sections were then deparaffinized, rehydrated in graded alcohol series, and stained with hematoxylin-eosin. The stained sections were imaged using a Nikon microscope (Ni-U, Nikon, Minato-ku, Japan) and analyzed using ImageJ software. For sperm morphological analyses, cauda epididymal sperm from control and high-Hcy mice were spread onto glass slides and air-dried. Sperm smears were stained with hematoxylin and eosin followed by microscopic examination.

Whole-genome bisulfite sequencing (WGBS) mapping and relative analysis

Genomic sperm DNA from the control group (n = 3) and Hcy-treated group (n = 3) were extracted using the Easy Pure Genomic DNA Kit (EE101, Transgen Biotech, Beijing, China) for construction of WGBS libraries. In brief, gDNA was fragmented by sonication to about 200 bp in size. Fragmented DNA was end-repaired and ligated to methylated adapters, and a gDNA library was constructed according to the manufacturer's instructions (Illumina, California, USA). Unmethylated cytosines were converted to uracils by bisulfite treatment. The converted DNA was subjected to 150-bp paired-end WGBS sequencing performed on an Illumina Hiseq X at Annoroad Gene Technology Company (Beijing, China). For WGBS data analysis, low-quality reads were filtered. Methylation degrees were calculated as mC/(mC + C). For further analysis, quality control and read trimming were conducted by using fastp. Subsequently, clean fastq data were mapped to the mouse reference genome (mm10 assembly) using bsmap. The resulting SAM format data by bsmap were converted and sorted by samtools. The DNA methylation sites were called using BSseeker2. The differential methylation sites and regions were identified by R/Bioconductor methylKit package. In total, 121 CHD-related genes, which were reported before, were selected in DNA methylation analysis. Absolute methylation differences between groups were set to at least 10%, and $p < 0.05$ was then considered as the DMR.

QUANTIFICATION AND STATISTICAL ANALYSIS

Statistical analysis was performed by using GraphPad Prism8. Statistical significance was determined by unpaired two-tailed t-test, unpaired t test with Welch's correction, chi-square with/with correction test and Fisher's exact test NS (not significant), *, **, and ***, represent $p > 0.05$, $p \leq 0.05$, $p \leq 0.01$, and $p \leq 0.001$, respectively.